Am J Transl Res 2023;15(4):2389-2406
www.ajtr.org /ISSN:1943-8141/AJTR0148601

Original Article

Buyang huanwu decoction (BYHWD) alleviates sepsis-induced myocardial injury by suppressing local immune cell infiltration and skewing M2-macrophage polarization

Lingling Xiao[1*#], Xixiang Xi[1*], Meng Zhao[2], Lifen Zhang[1#], Kai Zhang[3#], Zhenyu Xu[1#]

[1]Department of Emergency Medicine, Emergency Intensive Care Unit, Shanghai Seventh People's Hospital, The Seventh People's Hospital Affiliated to Shanghai University of Traditional Chinese Medicine, 358 Datong Road, Pudong, Shanghai 200137, China; [2]Department of Otolaryngology Head and Neck Surgery, Children's Hospital of Fudan University, 399 Wanyuan Road, Minhang, Shanghai 201102, China; [3]State Key Laboratory of Oncogenes and Related Genes, Renji-Med-X Stem Cell Research Center, Ren Ji Hospital, Shanghai Cancer Institute, Shanghai Jiao Tong University School of Medicine, 160 Pujian Road, Pudong, Shanghai 200127, China. [*]Equal contributors. [#]Senior authors.

Received December 18, 2022; Accepted March 15, 2023; Epub April 15, 2023; Published April 30, 2023

Abstract: Objective: To investigate the therapeutic effect of Buyang huanwu decoction (BYHWD) on sepsis-induced myocardial injury (SIMI) and explore the mechanism by which BYHWD mitigates SIMI. Methods: The Lipopolysaccharide (LPS)-induced SIMI mouse model was established to detect the effect of BYHWD-low (1 mg/kg), BYHWD-middle (5 mg/kg), and BYWHD-high (20 mg/kg) on SIMI. The survival of these BYHWD-treated septic mice was investigated. The histology of myocardial tissues was determined by hematoxylin and eosin (H&E) staining. The apoptotic index and inflamed microenvironment of myocardial tissues were assessed by immunofluorescent staining (IF) and flow cytometry analysis. Liquid chromatography-mass spectrometry (LC-MS/MS) was employed to determine the key chemical components in the serum of BYHWD-loaded septic mice. Immunoblotting assay was utilized to detect NF-κB and TGF-β signaling activity, and M1/M2-macrophage markers using RAW264.7 cells. Results: The high dosage of BYHWD (BYHWD-high, 20 mg/Kg) significantly attenuated SIMI and improved the survival of septic mice. The BYHWD-high solution markedly reduced myocardial cell apoptosis and mitigated the inflamed microenvironment by suppressing $CD45^+$ immune cell infiltration. Importantly, BYHWD decreased macrophage accumulation and promoted an M2-macrophage polarization. Paeoniflorin (PF) and calycosin-7-O-β-glucoside (CBG) were identified as the key molecules in BYWHD with therapeutic effect. PF (10 μM) and CBG (1 μM) inhibited NF-κB signaling, meanwhile they upregulated the TGF-β pathway, thereby facilitating an M2-macrophage phenotypic transition in RAW264.7 cells. Conclusions: BYHWD, with two effective components PF and CBG, can mitigate SIMI by suppressing the inflamed myocardial microenvironment and skewing an immunosuppressive M2-macrophage phenotype.

Keywords: Buyang huanwu decoction (BYHWD), sepsis-induced myocardial injury (SIMI), inflamed microenvironment, M2-macrophage, NF-κB signaling, TGF-β signaling

Introduction

Sepsis is a severe complication caused by injuries, such as trauma, burns, surgery, and infections [1]. As a key feature of sepsis, uncontrollable inflammation often leads to multiple organ disorders [2]. Heart dysfunction, in particular, sepsis-induced myocardial injury (SIMI) has been regarded as a critical contributor to septic mortality [3]. Currently, identification of the molecular mechanism by which myocardial tissue is damaged in septic patients has become a hotspot of clinical and pre-clinical studies.

The lipopolysaccharide (LPS)-induced septic mouse model with myocardial injury is frequently utilized for mechanism investigation and druggable target screening [4-6]. Using this model, several important mechanisms underlying SIMI have been revealed. For example, the elevated production of proinflammatory cyto-

kines, dysregulated calcium homeostasis, increased amount of reactive oxygen species (ROS), and impaired mitochondrial function can result in myocardial cell apoptosis and death [7]. Indeed, based on these cytological mechanisms, several clinical managements, for instance, restriction of infection source, providing myocardial function support, and cardiac protective agents alleviate SIMI to some extent [8-10]. However, the mortality of septic patients remains high [11]. To optimize clinical intervention and improve prognosis of septic patients, we need to further explore unknown cellular and molecular mechanisms, investigate novel druggable targets, and screen new drugs.

The increased proinflammatory cytokines including interleukin 1β (IL-1β), IL-6, and tumor necrosis factor (TNF-α) are usually generated by immune cells [12-14]. Interestingly, a recent study has demonstrated that myocardial cells *per se* are able to produce cytokines under stressed conditions [15]. Based on this finding, it is reasonable to speculate that these locally produced cytokines may boost an inflamed cardiac microenvironment in septic patients. Moreover, myocardial fibrosis also enables upregulated cytokine production, and thereby creates an inflamed myocardial milieu [16, 17]. These inspiring studies prompt us to raise an interesting question of whether these locally produced cytokines can inflame the myocardial microenvironment, promote myocardial cell apoptosis, and eventually accelerate disease progression. To address these unsolved issues may be helpful to interrogate new druggable targets for SIMI from a novel perspective.

Traditional Chinese medicine (TCM) has been widely used in China and other Asian countries throughout history. Recently, TCM has started to fit into the settings of western medicine, not merely limited to a supportive role. As a renowned TCM prescription, Buyang huanwu decoction (BYHWD) consists of seven herbs including Huangqi (Astragali Radix), Danggui (Angelicae Sinensis Radix), Chishao (Paeoniae Radix Rubra), Chuanxiong (Chuanxiong Rhizoma), Taoren (Persicae Semen), Honghua (Carthami Flos), and Dilong (Pheretima) at a ratio of 120:6:4.5:3:3:3:3 with their dry weights [18]. BYHWD has been broadly applied for clinical treatment of stroke [19], neuronal injury [20, 21], atherosclerosis [22], and cardiovascular and cerebrovascular disorders [23]. Mechanistically, BYHWD involves in a wide spectrum of cell signaling pathways in a context-dependent manner. For instance, BYHWD activates the vascular endothelial growth factor (VEGF) signaling in a cerebral ischemia mouse model [24]. In addition, BYHWD promotes bone marrow mesenchymal stem cells differentiation by activating mitogen-activated protein kinase (MAPK) signaling [25]. Of note, the anti-inflammatory effect of BYHWD has been widely demonstrated in distinct scenarios [26, 27]. A recent study reported that BYHWD ameliorates atherosclerosis by promoting regulatory T cell (Treg) differentiation [22]. However, to the best of our knowledge, the therapeutic effect of BYHWD on SIMI has not been addressed so far.

Herein, we aim to investigate the therapeutic effects of BYHWD on SIMI with an LPS-induced septic mouse model. From a novel perspective, we bridge a previously unknown knowledge gap that BYHWD can mitigate myocardial injury by suppressing the inflamed myocardial microenvironment and skewing macrophagse toward an M2-biased polarization.

Material and methods

Preparation of BYHWD solution

The herbs of BYHWD were obtained from the Shanghai Seventh People's Hospital with dry weights of Astragali Radix 120 g, Angelicae Sinensis Radix 6 g, Paeoniae Radix Rubra 4.5 g, Chuanxiong Rhizoma 3 g, Persicae Semen 3 g, Carthami Flos 3 g, Pheretima 3 g. These herbs were confirmed by Dr. Jing-Hua Ye, a renowned TCM expert now working at Shanghai Seventh People's hospital. All these botanical mixtures were transferred to a beaker with 1 L distilled water and boiled twice at 100°C for 60 min. In detail, the drug solution was collected after the first round of boiling, and solid residues were resuspended with water and boiled again similarly. The solutions from two rounds of boiling were combined for condensation at 65°C with a rotary evaporator. The concentrated drug solution was subsequently vacuum-cooled, dried, and made into solid powder, which was dissolved in distilled water to generate the original BYHWD solution with a final concentration of 1.5 g/mL. The BYHWD solution was aliquoted and stored at -20°C. In animal experiments, the original BYHWD solution was further diluted into BYHWD-low (1 mg/Kg), BYHWD-middle (5 mg/Kg), and BYHWD-high (20 mg/Kg) based on the body weight of mice.

Animal experiments

Eight week-old wild type (WT) C57BL/6 male mice were purchased from Beijing SPF Co. Ltd. To establish the LPS-induced septic mouse model, mice were intraperitoneally (i.p.) injected them with LPS (5 mg/kg). The peripheral blood was collected after LPS injection, and cytokines including IL-1β, IL-6, and TNF-α were determined using ELISA assay. To assess the effect of BYHWD on mice, low, middle, and high dosages of BYHWD solution were intragastrically (i.g.) administrated once per day for a week. After BYHWD treatment, the body weight was measured. One week later, the major organs including the heart, liver, kidney, and lung were collected for histological analysis. To assess therapeutic effects of BYHWD, LPS was administered via i.p. injection into these mice. The septic mice were then randomly separated into four groups. The vehicle (phosphate buffered solution, PBS), BYHWD-low, BYHWD-mid, and BYHWD-high solutions were i.g. administrated once *per* day into these mice for a week. The survival was depicted accordingly.

In vitro hemolytic assay

A total of 2 mL blood was collected from C57BL/6 mice via cardiac puncture. We stirred the blood with a glass rod to remove the fibrinogen. Eighteen mL 0.9% NaCl solution was added into the fibrinogen-free-blood. The mixture was centrifuged at 1,500 rpm for 15 min at room temperature (RT). We removed the supernatant carefully and kept the red blood cell (RBC) pellet in the bottom of the tubes. Next, we washed the RBC with 0.9% NaCl and spun down until the supernatant become clear. The pellets were resuspend with 0.9% NaCl to generate 2% (v/v) RBC suspension. NaCl, 0.9% serves as a negative control. The distilled water was used as positive control. The diluted BYHWD was incubated with equal volume of 2% RBC suspension at 37°C for 3 hours (h). To assess the hemolytic rate (HR), the $OD_{545\ nm}$ values were determined using a microplate reader (Elx800, BioTek). The HR is calculated with the formula:

$HR = (OD_{545\ nm}$ sample - $OD_{545\ nm}$ negative control)/($OD_{545\ nm}$ positive control - $OD_{545\ nm}$ negative control) × 100%

Liquid chromatography and mass spectrometry (LC-MS/MS) analysis

The serum of BYHWD-loaded septic mice was collected and mixed with 10 μL liquiritin (10 μg/mL) and 400 μL methanol. The mixture was then centrifuged at 12,000 rpm at 4°C for 10 min. The supernatant was collected and dried with nitrogen. We added 100 μL methanol into the tube and dissolved the sample. The sample was centrifuged at 12,000 rpm at 4°C for 10 min. Five μL sample was used for further LC-MS/MS analysis. Similarly, 100 μL serum from untreated normal mice were prepared. The LC-MS/MS analysis was performed using the Agilent 1200 system (Agilent Corp., USA) and triple-quadrupole mass spectrometer (API 3200, Canada). Electrospray ionization (ESI) was performed in positive and negative ionization mode.

Hematoxylin and eosin (H&E) and immunofluorescence (IF) staining

Paraffin-embedded sections of myocardial tissues were deparaffinized, rehydrated and stained with H&E solutions. For IF assay, the deparaffinized and rehydrated slides were boiled with antigen retrieval buffer (10 mM citrate buffer, pH = 6.0) for 10 min using a microwave oven. Slides were incubated in blocking buffer (10% goat serum in PBS) with 0.1% Triton X-100 for 1 h at RT. Primary antibodies were used to incubate the slides at 4°C overnight. All primary antibodies including Col1a1 (Cell signaling, #81375), αSMA (Cell signaling, #19245), cleaved caspase 3 (CC3, cell signaling, #9661), γH2AX (Cell signaling, #60566), and CD45 (Cell signaling, #70257) were diluted at 1:300 for IF staining assay. Slides were incubated with secondary antibodies for 1 h at RT. The secondary antibodies were removed and counterstained with 4',6-diamidino-2-phenylindole (DAPI) for 5 min at RT. The stained sections were examined using a fluorescence microscope. Images were captured and analyzed by Image J software.

ELISA assay

The blood samples were collected from mice through cardiac puncture. The blood was transferred into 1.5 mL Eppendorf tubes and placed at RT for 30 min. After centrifuging, the plasma supernatants were frozen in liquid nitrogen and

stored at -80°C. IL-1β, IL-6, IL-10, TNF-α and TGF-β were determined using a commercial ELISA kit (Quantikine ELISA lit, R&D system, USA).

Immunoblotting analysis

The myocardial tissues from mice were collected and homogenized using a tissue lyzer (Tissuelyzer II, QIAGEN, Germany) in lysis buffer (150 mM NaCl, 300 mM sucrose, protease and phosphatase inhibitors (PIs), and 20 μM streptozotocin (pH 8.0)). Cells were further lysed with NP-40 buffer (150 mM NaCl, 50 mM Tris-HCl (pH 8.0), 0.5% NP-40, PIs). RAW264.7 cells were subsequently lysed and centrifuged at 12,000 rpm for 30 min at 4°C and transferred to new tubes. Samples were loaded and separated by SDS-PAGE and transferred to nitrocellulose (NC) membrane (GE Healthcare Life Science, Germany). The NC membranes were incubated with 5% skimmed milk at RT. Primary antibodies (Supplementary Table 1) were probed at 4°C overnight. The NC membranes were incubated with horseradish peroxidase conjugated secondary antibodies for 1 h at RT. The protein bands were detected by the Enhanced Chemiluminescent (ECL) detection system.

Quantitative polymerase chain reaction (RT-qPCR) analysis

Total RNA was extracted using the Takara RNA isolation kit. The detailed protocols were strictly followed by manufacturer's guidance. Briefly, 500 ng RNA was reversely transcribed using Takara Prime Script TM RT reagent Kit (Takara, Japan). The cDNA was amplified with specific primers (Supplementary Table 2). The relative gene expression was calculated using the $2^{-\Delta\Delta CT}$ method.

Flow cytometry

The myocardial tissues were minced and digested by DNase I, collagenase and trypsin for 2 h at 37°C. The samples were then filtered through 70 μm cell strainers and centrifuged at 300 g for 5 min at RT. The cell pellets were resuspended to generate a single cell suspension. The samples were detected using BD LSR Fortessa instrument. The data were analyzed by Flow Jo software.

Cell culture

The RAW264.7 cells were commercially obtained from American type culture collection (ATCC). Cells were cultured in Dulbecco's modified Eagle's medium (DMEM, Hyclone, USA) supplemented with 5% FBS (Hyclone, USA), 1% penicillin and streptomycin (Hyclone, USA) at 37°C in 5% CO_2 humidified atmosphere incubator.

Statistical analysis

Data are displayed as the mean with standard error from independent experiments. Statistical differences between the two groups were analyzed by student's *t*-test. The survival was analyzed using log rank test. The statistical analysis of the data was performed using GraphPad Prism 8 software.

Results

BYHWD exhibits low hemolytic and toxic activities in mice

The constituents of BYHWD were shown in Supplementary Table 3, where their Chinese name, English name, Latin name, and dry weight were provided. These herbs were mixed, boiled, baked, condensed, and eventually made into original BYHWD solution with a concentration of 1.5 g/mL (**Figure 1A**). We firstly assessed the hemolytic effect of BYHWD on mice. The BYHWD solution was diluted into a wide range of concentrations from nanogram (ng/mL) to milligram (mg/mL) scale. As a result, no detectable hemolytic effect was identified (**Figure 1B**). Based on a previous study [22], three dosages of BYHWD solution including low, middle, and high were prepared. As shown in **Figure 1C**, the hemolytic rates of all dosages were less than 5%, suggesting little hemolytic effect. We examined mouse body weight before and after BYHWD treatment and did not find evident alterations (**Figure 1D**). H&E staining showed that there was no histological change within the major organs between control (PBS) and BYHWD treated mice (**Figure 1E**). Therefore, BYHWD exhibits biosafety with no hemolytic or toxic activities in C57BL/6 mice.

BYHWD shows therapeutic effects on LPS-induced septic mice

We next assessed the therapeutic effect of BYHWD on LPS-induced septic mice. Septic

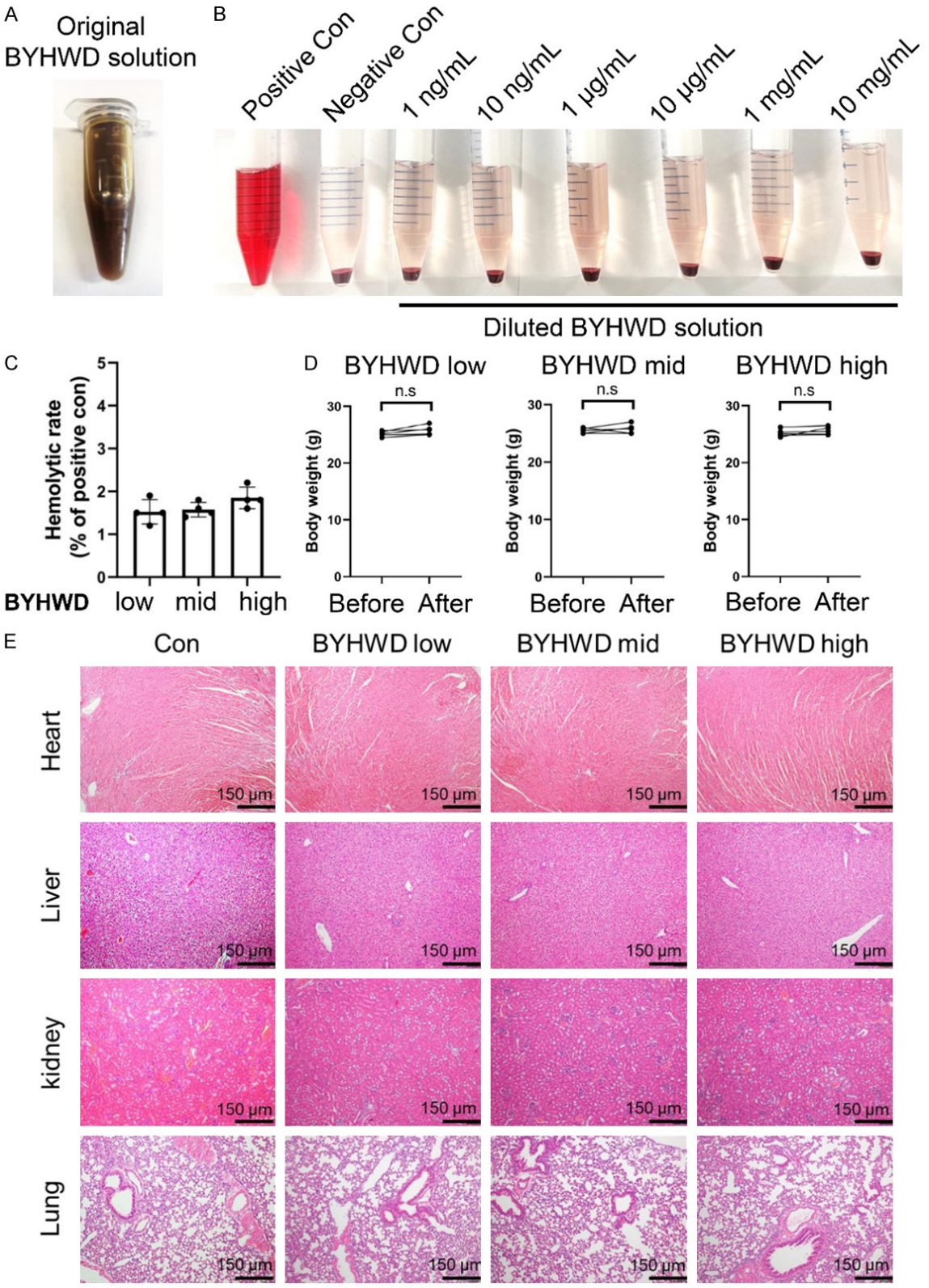

Figure 1. BYHWD shows extremely low hemolytic and toxic activities in mice. A. The original BYHWD solution (1.5 g/mL). B. The *in vitro* hemolytic assay showing that BYHWD has no detectable hemolytic effect. The 0.9% NaCl solution is used as a negative control, and distilled water serves as a positive control. C. Quantification of the hemolytic rate of BYHWD-low, BYHWD-mid, and BYHWD-high-treated mice (n = 4). D. Measurement of the body weight before

and after BYHWD treatment with different dosages (n = 5). Mice were treated for one week. Student's *t*-test. n.s = non-significant. E. H&E staining images reveal histological morphologies of major organs including the heart, liver, kidney, and lung from vehicle-treated mice and BYHWD-low, BYHWD-mid, and BYHWD-high treated mice (n = 5). Scale bar = 150 μm. n.s = non-significant.

mice were randomly separated into four groups that were treated with vehicle (PBS), BYHWD-low, -middle, and -high solutions for one week. Their survival was monitored for two weeks. As a result, BYHWD benefited the survival of septic mice in a dose-dependent manner (**Figure 2A**). Normal mice displayed intact cardiac stripes, integrated myocardial membrane, and clear cellular and tissue morphology (**Figure 2B**). However, the septic mice showed damaged cardiac structure and disrupted myocardial membrane (**Figure 2C**). Intriguingly, BYHWD-treated septic mice (**Figure 2D-F**), particularly, the middle (**Figure 2E**) and high (**Figure 2F**) dosage treated mice displayed markedly attenuated tissue damages. Of note, BYHWD significantly decreased myocardial injury index (**Figure 2G**) and restored heart weight (**Figure 2H**). These data demonstrated that BYHWD benefits the survival and mitigates SIMI. Considering the high dosage of BYHWD displayed the most profound therapeutic effect, we utilized the BYHWD-high solution to perform experiments hereafter.

BYHWD reduces myocardial fibrosis and apoptosis in septic mice

Myocardial fibrosis is frequently detected in cardiac injury [28]. As a key feature of inflamed myocardial tissues, fibrosis was clearly detected by increased collagen deposition (**Figure 3A**). Compared with normal mice, septic mice showed evident myocardial fibrosis, reflected by increased Collagen type I α chain I (Col1a1) and α smooth muscle actin (αSMA) (**Figure 3B**). The quantification of Cal1a1$^+$ (**Figure 3C**) and αSMA$^+$ myocardial cells (**Figure 3D**) indicated that BYHWD prohibits myocardial fibrosis in septic mice. Inflammation usually causes apoptosis. IF staining showed increased apoptotic myocardial cells, featuring with elevated cleaved-caspase 3 (CC3$^+$) positive cells in septic mice (**Figure 4A**). BYHWD significantly reduced CC3$^+$ cells in myocardial tissues of septic mice (**Figure 4B**). Annexin-V staining confirmed that BYHWD can strongly decrease myocardial cell apoptosis (**Figure 4C**, **4D**). These results revealed that BYHWD can markedly mitigate apoptosis in myocardial tissues of septic mice.

BYHWD represses overall inflammation and attenuates inflamed myocardial microenvironment in septic mice

We collected blood from normal mice, vehicle, and BYHWD-treated septic mice, and found that BYHWD significantly decreased the circulating IL-1β (**Figure 5A**), IL-6 (**Figure 5B**), IL-12 (**Figure 5C**) and TNF-α (**Figure 5D**) in septic mice. On the contrary, transformation growth factor-β (TGF-β) (**Figure 5E**), a classic immunosuppressive cytokine [30], was increased upon BYWHD treatment. In addition to overall inflammatory status reflected by cytokines in the circulation, we next sought to assess the myocardial immune microenvironment in septic mice. Flow cytometric analysis detected very rare CD45$^+$ cells in the heart of normal mice, but in septic mice this ratio markedly increased, suggesting an inflamed microenvironment (**Figure 6A**). Upon BYHWD treatment, the increased CD45$^+$ cells were dropped to a comparable level in normal mice. IF staining validated the inhibitory effect of BYHWD on the inflamed myocardial microenvironment in which immune cell infiltration was repressed (**Figure 6B**, **6C**). Immune cell components and their proportions in myocardial tissues of septic mice were interrogated. Surprisingly, macrophages took up over 50% in the local immune landscape, serving as the most abundant leucocyte (**Figure 6D**). These data suggested that macrophages may play a major role in myocardial tissue homeostasis of septic mice.

BYHWD decreases macrophage proportion and promotes M2-macrophage polarization

To test whether BYHWD impacts macrophage proportions in myocardial tissues of septic mice, the macrophage/CD45$^+$ ratio of normal mice, and vehicle, and BYHWD treated septic mice were assessed. As shown in **Figure 7A**, **7B**, BYHWD decreased the macrophage/CD45 ratio from 44.8% to 28.1%. Macrophages can be conventionally divided into proinflammatory

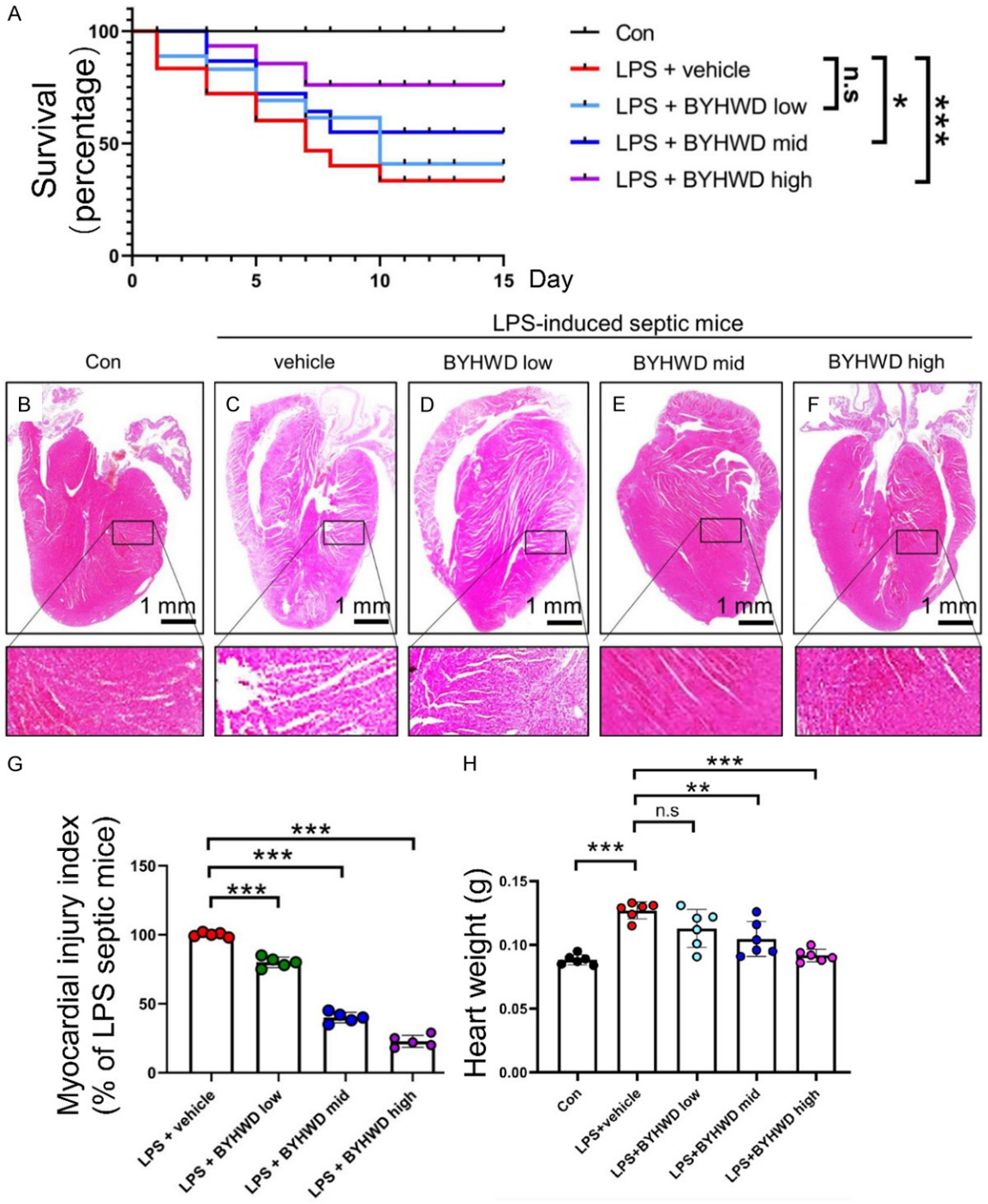

Figure 2. BYHWD benefits survival and attenuates myocardial injury in LPS-induced septic mice. (A) The survival curves of normal mice (Con), and vehicle, BYHWD-low, BYHWD-mid, and BYHWD-high treated septic mice (n = 15 for each group). Log rank test. $^{*}P < 0.05$; $^{***}P < 0.001$. (B-F) H&E staining showing the histology of myocardial tissues of normal mice (Con) (B), vehicle-treated septic mice (C), BYHWD-low (D), BYHWD-mid (E), and BYHWD-high treated septic mice (F). Scale bar = 1 mm. (G) The myocardial injury index was quantified based on the crack number presented in the myocardial tissues of vehicle, BYHWD-low, BYHWD-mid, and BYHWD-high treated septic mice (n = 5). Student's *t*-test. $^{***}P < 0.001$. (H) The heart weight of normal (Con) mice, and vehicle, BYHWD-low, BYHWD-mid, and BYHWD-high treated septic mice (n = 6). Student's *t*-test. $^{*}P < 0.05$; $^{**}P < 0.01$; $^{***}P < 0.001$; n.s = non-significant.

M1 and immunosuppressive M2-macrophages [31]. A set of marker genes were employed to make M1 distinct from M2-macrophages [32]. Using fluorescence activated cell sorting

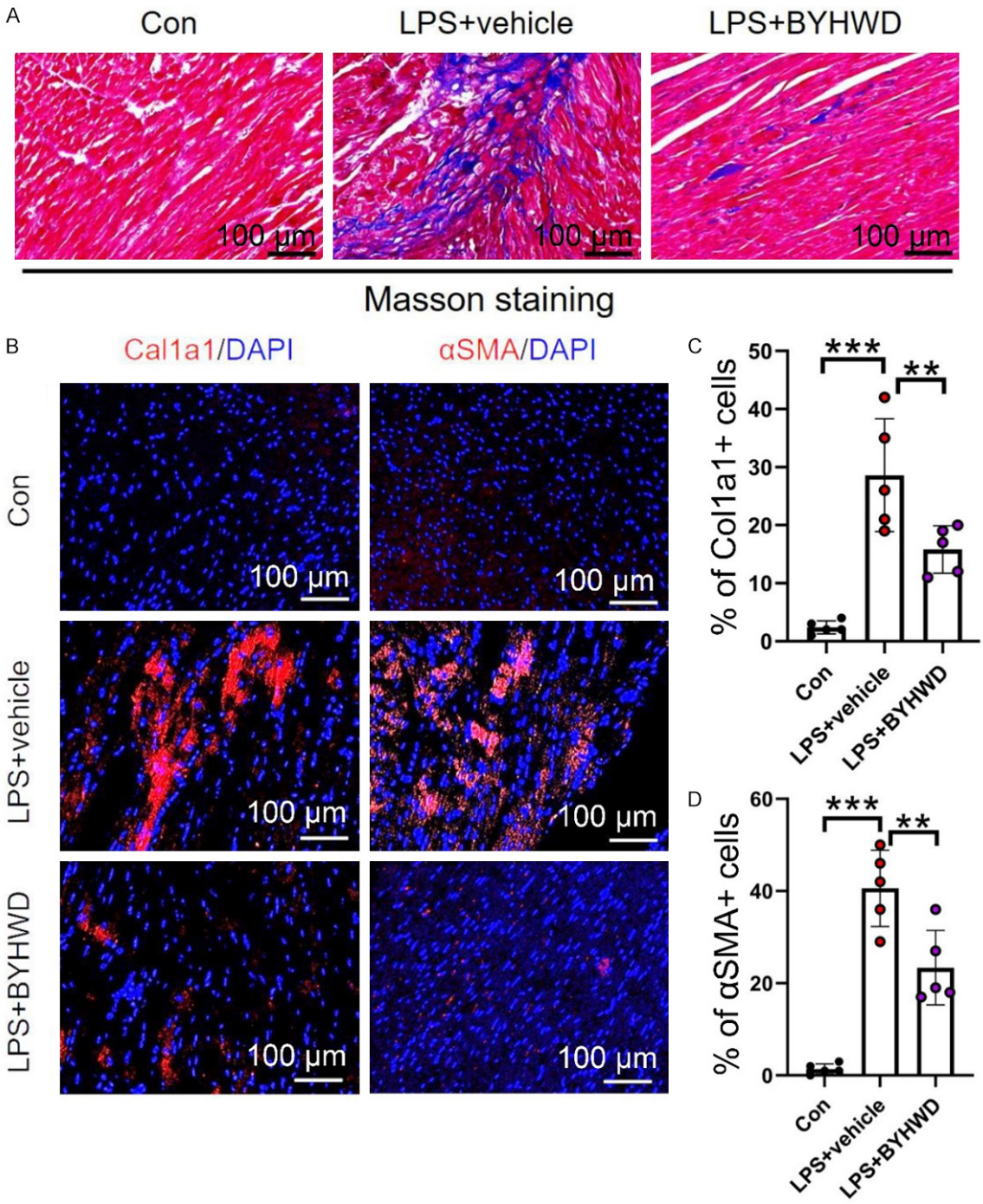

Figure 3. BYHWD alleviates myocardial fibrosis in septic mice. (A) Masson staining demonstrates the collagen disposition (blue color) in myocardial tissue. Scale bar = 100 μm. (B) IF staining images showing fibrosis markers including Collagen type I α chain I (Col1a1) and α smooth muscle actin (αSMA) in myocardial tissues of control mice, vehicle and BYHWD-high treated septic mice. Nuclei were counterstained with 4',6-diamidino-2-phenylindole (DAPI). Scale bar = 100 μm. (C, D) Quantification of the percentage of Col1a1^{+} (C) and αSMA^{+} (D) myocardial cells. Results were shown as mean ± SEM, student's *t*-test, $^{**}P < 0.01$; $^{***}P < 0.001$.

(FACS)-isolated macrophages from myocardial tissues, we found that BYHWD strongly decreases the expression of M1-macrophage markers including *Tnfa* (**Figure 8A**), *H2Aa* (**Figure 8B**), and *Nos2* (**Figure 8C**). On the other hand, M2-macrophage marker genes, such as *Cd163*

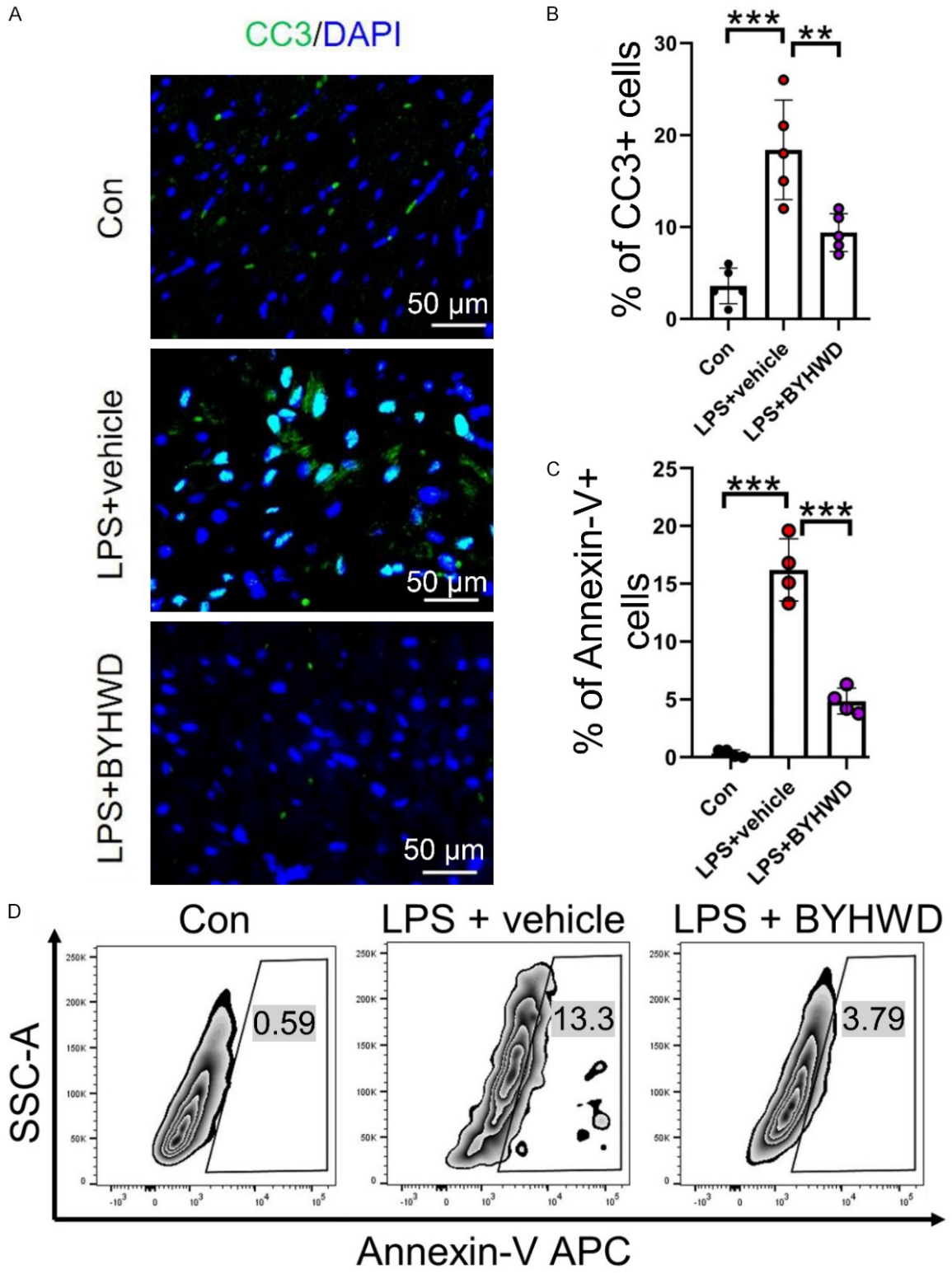

Figure 4. BYHWD inhibits myocardial cell apoptosis in septic mice. A. IF staining images revealing the expression of cleaved-caspase 3 (CC3) in myocardial tissues of normal mice (Con), vehicle and BYHWD-high treated septic mice. Nuclei were counterstained with DAPI. Scale bar = 50 μm. B. Quantification of the percentage of CC3 expressing myocardial cells based on IF staining data (n = 5). Student's *t*-test, $^{**}P < 0.01$; $^{***}P < 0.001$. C. Quantification of the percentage of Annexin-V expressing myocardial cells based on flow cytometry data (n = 4). Student's *t*-test, $^{***}P < 0.001$. D. Flow cytometric analysis showing the ratio of Annexin-V$^+$ cells in myocardial tissues of normal mice (Con), vehicle and BYHWD-high treated septic mice.

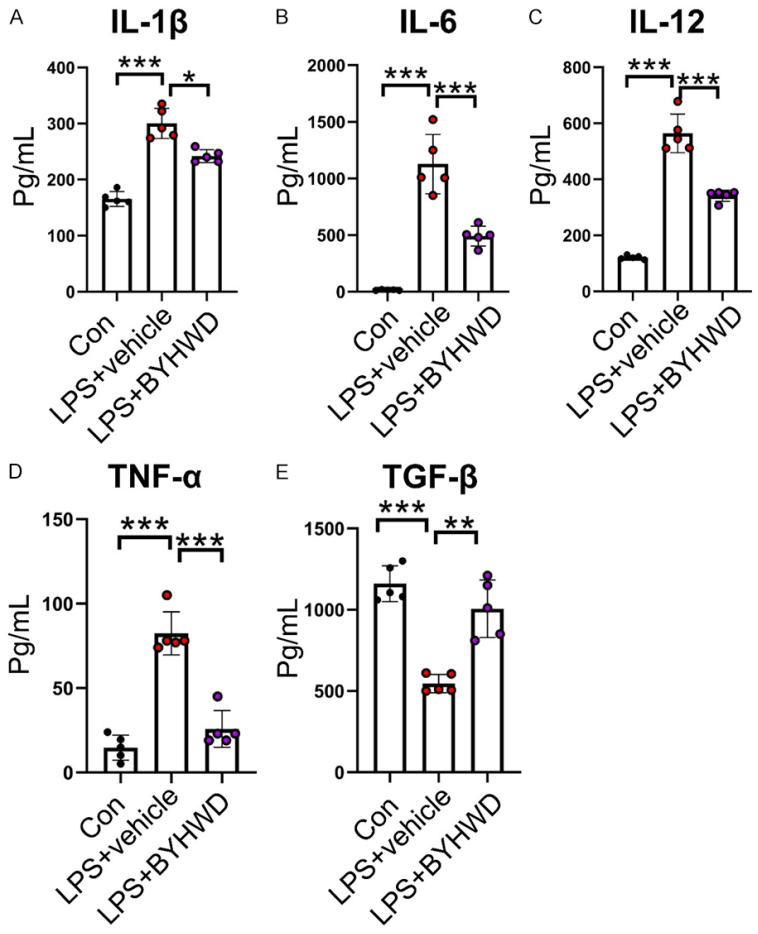

Figure 5. BYHWD suppresses proinflammatory cytokines in the peripheral blood of septic mice. (A-E) ELISA results showing that BYHWD can decrease the level of proinflammatory cytokines including IL-1β (A), IL-6 (B), IL-12 (C) and TNF-α (D) but increase immunosuppressive cytokine TGF-β (E) in the blood of septic mice. Data were shown as ± SEM, Student's *t*-test. $^{*}P < 0.05$; $^{**}P < 0.01$; $^{***}P < 0.001$.

(**Figure 8D**), *Cd206* (**Figure 8E**), and *Arg1* (**Figure 8F**) were significantly elevated upon BYHWD treatment. Collectively, BYHWD not only decreases macrophage/CD45 proportion, but also promotes an M2-biased polarization.

Paeoniflorin (PF) and calycosin-7-O-β-glucoside (CBG) were identified in the serum of BYHWD-loaded mice

We next explored the major chemical components that may play roles in BYHWD-alleviated myocardial injury. To this end, the serum of BYHWD-loaded septic mice were collected for LC-MS/MS analysis (**Figure 9A**). Two most enriched chemical constituents were paeoniflorin (PF) (**Figure 9B**) and calycosin-7-O-β-glucoside (CBG) (**Figure 9C**). The PF is a major component from *Paeonia lactiflora* Pall, and the CBG was a constituent of *Astragalus. membranaceus* (Fisch.) Bge. var. *mongholicus* (Bge.) Hsiao [18]. A number of studies have well characterized the constituents in either BYHWD solution or the serum of BYHWD-treated animal [33, 34]. Interestingly, our results were in agreement with a previous study reporting the effect of BYHWD on atherosclerosis [22], in which, the four most enriched bioactive components were ononin, CBG, PF, and ferulic acid.

PF and CBG promote M2-macrophage polarization by orchestrating NF-κB and TGF-β signaling

To test whether BYHWD-mediated M2-macrophage polarization is reliant on PF or/and CBG, we employed a mouse monocyte/macrophage cell line RAW264.7 cells. The IC_{50} values of PF (**Figure 9D**) and CBG (**Figure 9E**) on RAW264.7 cells were assessed. To generate M1-macrophages, we pretreated RAW264.7 cells with LPS for 24 hr. These LPS-pretreated RAW264.7 were then stimulated by PF and/or CBG for 24 hr. Given that NF-κB signaling is critical for M1-macrophage polarization and TGF-β signaling is a key driver for M2-macrophage phenotypic transition, we determined whether PF and/or CBG can regulate these two signaling pathways. As shown in **Figure 9F**, both PF and CGB stimulation decreased phosphorylated p65 (p-p65) level. On the contrary, the p-Smad level was sharply increased in response to PF and CBF. Although PF and CGB did not repress the M1-macrophage marker iNOS, they elevated the classical M2-macrophage marker Arginase 1 (Arg1). To test whether PF and CGB have synergic effects on M2-macrophage polarization, we concomitantly treated RAW264.7 cells with these two molecules (**Figure 9G**). Upon combined PF and CGB

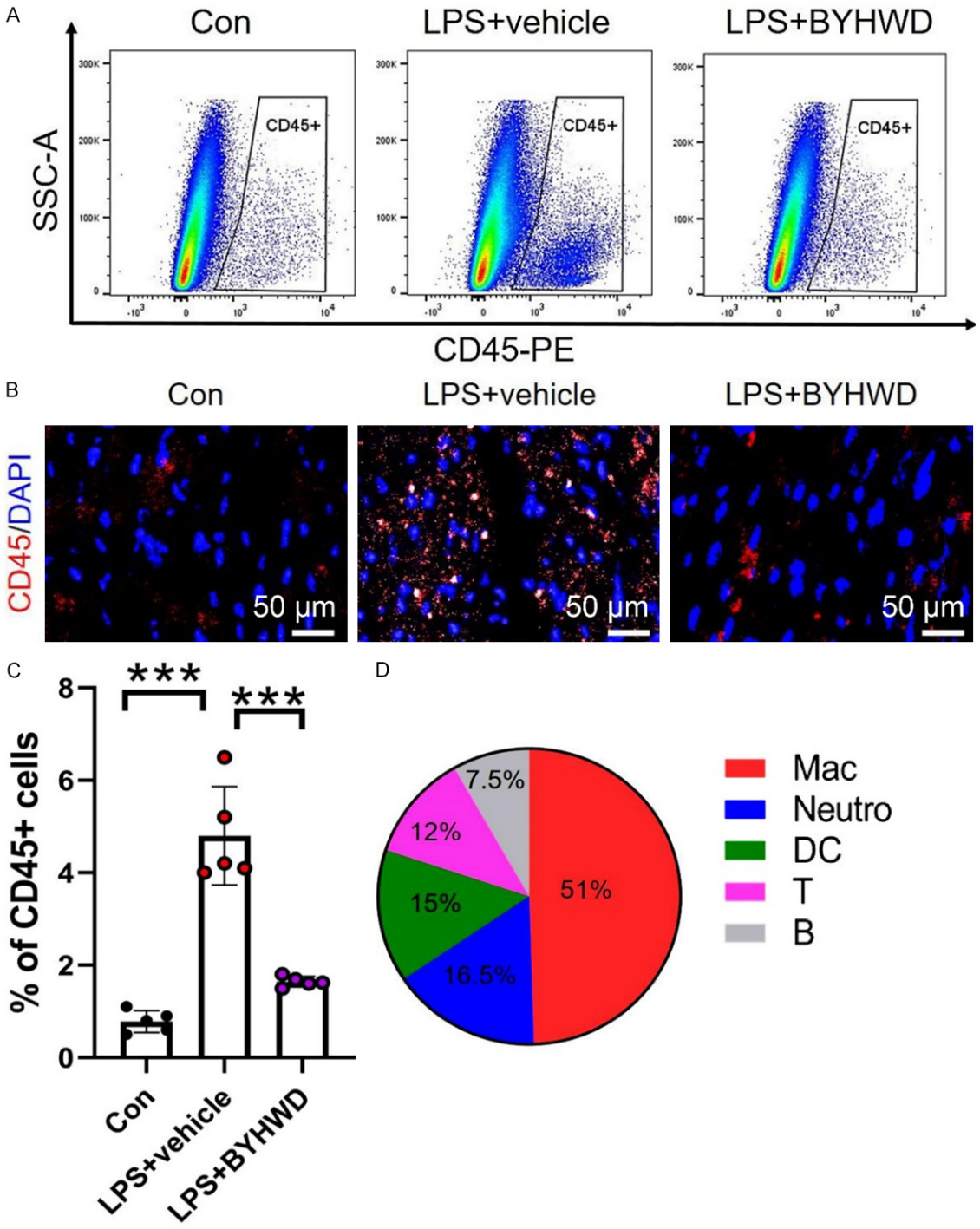

Figure 6. BYHWD decreases immune cell infiltration in the myocardial microenvironment of septic mice. A. Flow cytometry revealing the percentage of CD45$^+$ immune cell in myocardial tissues of normal (Con) mice, vehicle and BYHWD (high)-treated septic mice. B. IF staining images showing the CD45$^+$ immune cells in myocardial tissues of normal (Con) mice, vehicle and BYHWD (high)-treated septic mice. Nuclei were counterstained with DAPI. Scale bar = 50 μm. C. Quantification of CD45$^+$ immune cell proportions in myocardial tissues of normal (Con) mice, vehicle and BYHWD (high)-treated septic mice based on the flow cytometry results (n = 5). Student's *t*-test. $^*P < 0.05$; $^{**}P < 0.01$; $^{***}P < 0.001$. D. A pie chart demonstrating the proportion of macrophage (Mac), neutrophil (Neu), dentritic cell (DC), T and B cell in the inflamed myocardial tissue of LPS-induced septic mice.

stimulation, p-p65 and iNOS were all reduced. In contrast, p-Smad and Arg1 were elevated. However, the increased p-Smad and Arg1 were blocked by Poly I:C, an NF-κB/p65 agonist.

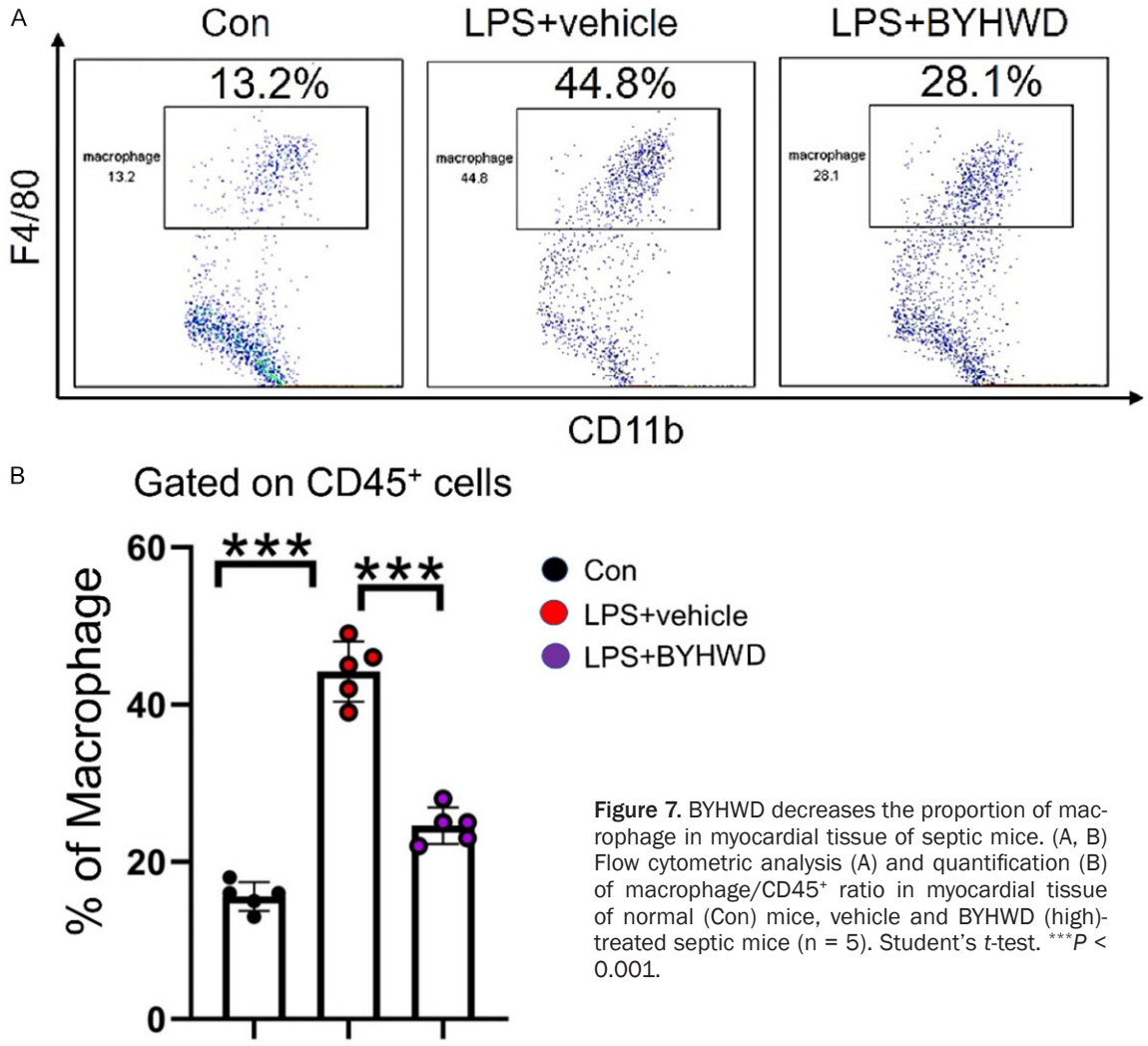

Figure 7. BYHWD decreases the proportion of macrophage in myocardial tissue of septic mice. (A, B) Flow cytometric analysis (A) and quantification (B) of macrophage/CD45$^+$ ratio in myocardial tissue of normal (Con) mice, vehicle and BYHWD (high)-treated septic mice (n = 5). Student's *t*-test. $^{***}P < 0.001$.

These data suggested that suppressed NF-κB signaling may be a prerequisite condition for M2-macrophage polarization.

PF and CBG alleviate SIMI and benefit septic mice survival

To validate the therapeutic effect of PF and CGB *in vivo*, we administrated them to LPS-induced septic mice. As shown in **Figure 10A**, both PF and CBG significantly improved the survival of septic mice, and they also attenuated myocardial injury (**Figure 10B**, **10C**). Using myocardial tissues of normal (Con) mice, vehicle, PF and CBG treated septic mice, immunoblotting data showed that either PF or CBG is sufficient to decrease IL-1β and TNF-α expression. They also decreased p-p65 but increased p-Smad level in septic mice (**Figure 10D**).

In summary, we found that BYHWD mitigates SIMI, in particular, represses the inflamed myocardial microenvironment by suppressing CD45$^+$ immune cell infiltration and skewing macrophages to an immunosuppressive M2 polarization. Using LC-MS/MS analysis, PF and CGB were identified as the two most abundant molecules in BYHWD-loaded serum of septic mice. These two molecules can drive the M2-macrophage phenotypic switch via orchestrating NF-κB and TGF-β signaling pathways (**Figure 10E**).

Discussion

For a long time, the locally inflamed microenvironment in myocardial tissues of septic patients has been not been vigorously investigated. Whether and how the inflamed microenviron-

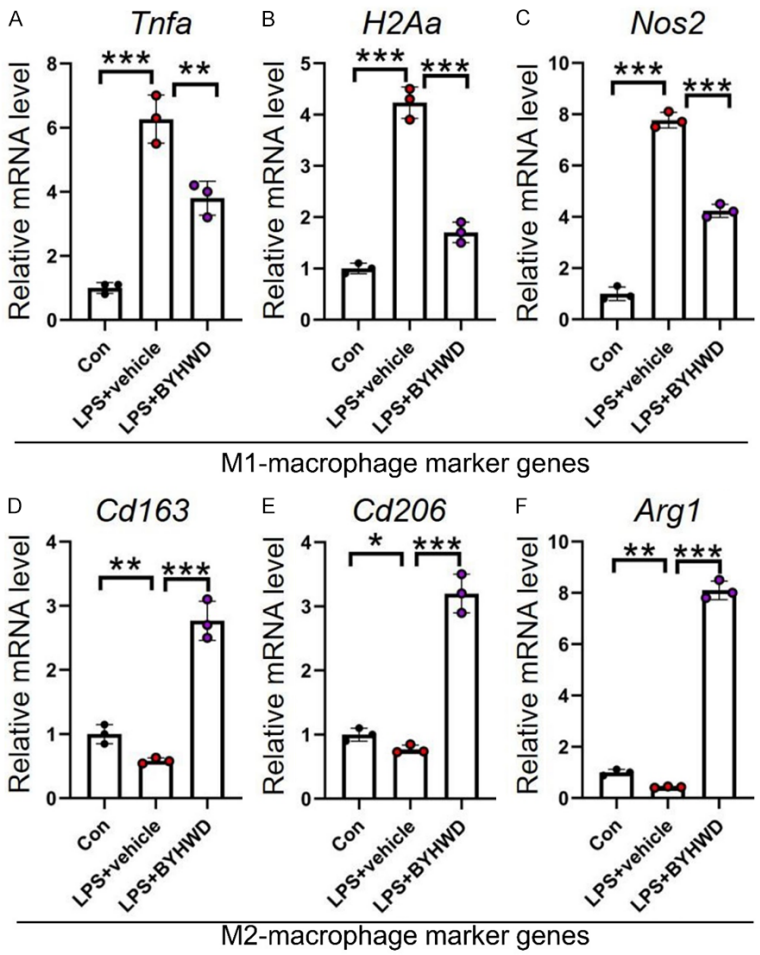

Figure 8. BYHWD promotes macrophages to gain an M2 phenotype in septic mice. (A-C) RT-qPCR assay determines the level of M1-macrophage marker genes including *Tnfa* (A), *H2Aa* (B), and *Nos2* (C) in FASC-sorted macrophages from myocardial tissues of normal (Con) mice, vehicle and BYHWD (high)-treated septic mice (n = 3). Student's *t*-test. $^{**}P < 0.01$; $^{***}P < 0.001$. (D-F) RT-qPCR data showing the expression of M2-macrophage marker genes including *Cd163* (D), *Cd206* (E), and *Arg1* (F) in FASC-isolated macrophages from myocardial tissues normal (Con) mice, vehicle and BYHWD (high)-treated septic mice (n = 3). Student's *t*-test. $^{*}P < 0.05$; $^{**}P < 0.001$; $^{***}P < 0.0001$.

ment promotes disease progression remains largely unknown. Here, with a widely used LPS-induced septic mouse model, we gained a better understanding of the inflamed myocardial microenvironment of septic hosts. In particular, we found an increased $CD45^+$ immune cell infiltration in the heart, and the major component of these $CD45^+$ cells are macrophages. Based on our results, the M2-polarized macrophage is helpful to counterbalance the inflamed microenvironment. Repressing the inflamed myocardial tissue benefits septic mice survival.

As a renowned TCM prescription, the anti-inflammatory effect of BYHWD has been well addressed by numerous literature. Here, we reveal a novel therapeutic function of BYHWD in mitigating SIMI. From a novel perspective, we uncover that BYHWD dampens the inflamed microenvironment in the heart of septic mice. Therefore, the effect of BYHWD on SIMI is achieved by restoring the inflamed microenvironment to a normal state.

With hundreds of bioactive molecules in BYWHD, it is reasonable to speculate that the effective compounds may vary in a context-dependent manner. In this study, we performed LC-MS/MS experiments and found that PF and CBG are the most enriched chemical components with longer retention in BYHWD-loaded serum. Interestingly, our results are in line with a very recent literature, in which, authors demonstrated that PF and CBG combined therapy mitigates ischemic stroke by activation of PI3K/AKT signaling [35], implying a broad therapeutic function of these two molecules. Mechanistically, these two compounds promote the M2-macrophage phenotypic transition by orchestrating NF-κB and TGF-β signaling.

Several recent investigations have reported therapeutic functions of BYHWD on heart disease. For example, BYHWD alleviates ischemic heart injury by decreasing circulating nitride oxide and cardiac CD40L expression [26]. Another study showed that BYHWD promotes angiogenesis and improves microcirculation in myocardial infarction [36-38]. These studies, in combination with our work, have provided a broad therapeutic potential of BYHWD in cardiac-related diseases, although the molecular mechanisms vary in details.

Collectively, we pinpoint that BYHWD acts as a promising TCM prescription to treat SIMI sep-

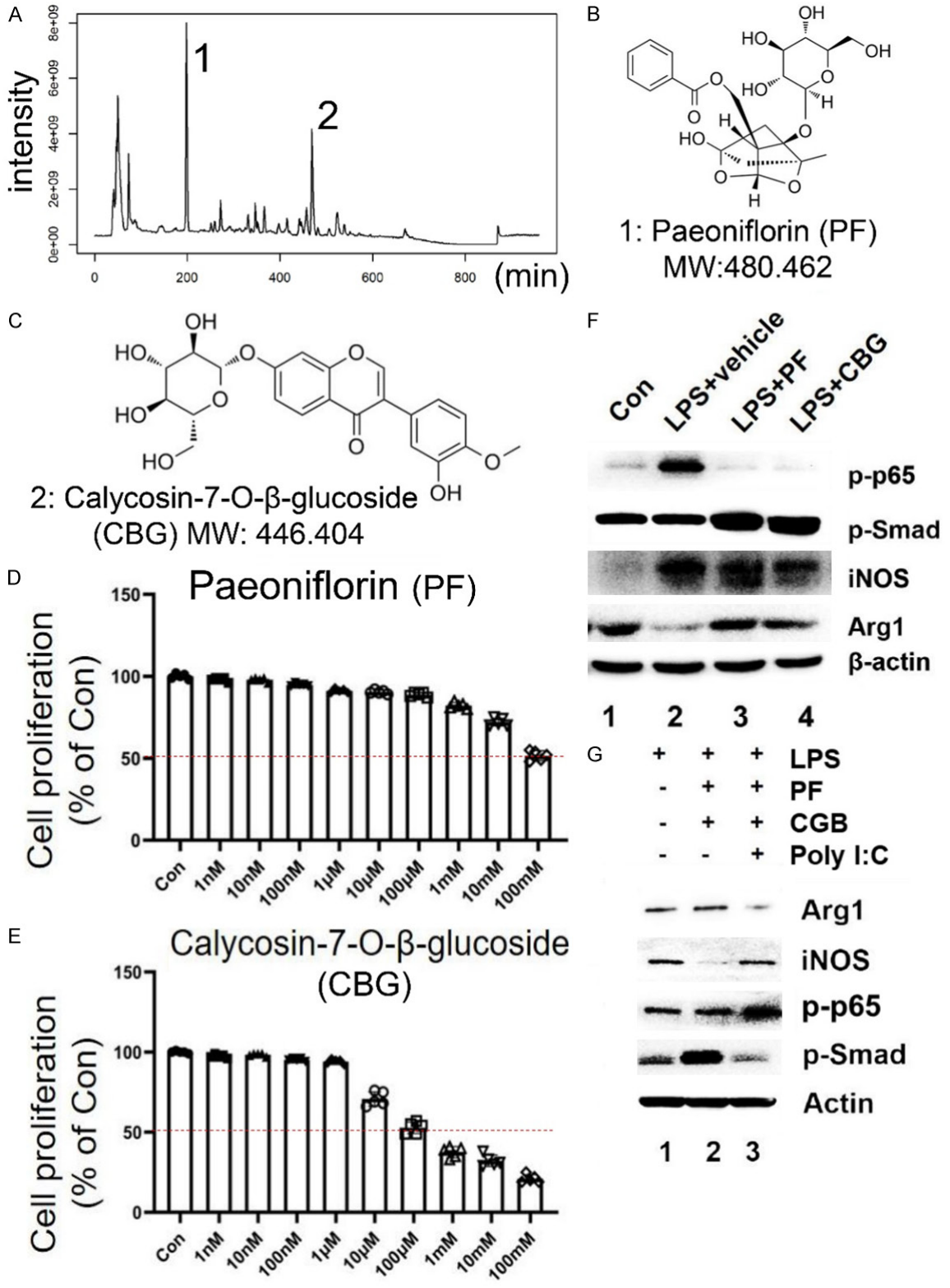

Figure 9. Paeoniflorin (PF) and calycosin-7-O-β-glucoside (CBG) are two key chemical components of BYHWD and drive M2-macropahge polarization by coordinating NF-κB and TGF-β signaling. (A) Liquid chromatography-mass spectrometry (LC-MS/MS) analysis of the serum from BYHWD-treated septic mice. The serum from normal mice served as control. The positive ion modes of LC-MS/MS were presented. Peak 1 and 2 indicate two most abundant chemical molecules of paeoniflorin (PF) and calycosin-7-O-β-glucoside (CBG). The representative sharp peaks of PF and CBG displayed here were detected in the diluted BYHWD solution. (B, C) Molecular structures and molecu-

lar weight of PF (B) and CBG (C). (D, E) Determination of the half maximal inhibitory concentration (IC_{50}) of PF (D) and CBG (E) using RAW264.7cells. (F) Immunoblotting of indicated proteins including phosphorylated p65 (p-p65), p-Smad, iNOS, arginase 1 (Arg1), and Actin. Untreated RAW264.7 cells serve as control (Con). RAW264.7 cells were pretreated with LPS (10 ng/mL, HY-D1056, MCE) for 24 hr. After LPS was removed, these cells were further stimulated by vehicle (DMSO), PF (10 μM, HY-0293, MCE), and CBG (1 μM, HY-N0520, MCE) for 24 hr before cells were collected. (G) Immunoblotting data showing the protein level of p-p65, p-Smad, iNOS, Arg1, and Actin. The RAW264.7 cells were pretreated with LPS (10 ng/mL) for 24 hr to acquire an M1-macrophage phenotype. After LPS was removed, these cells were further stimulated by either PF (10 μM) or CBG (1 μM) individually or in a combined manner for 24 hr.

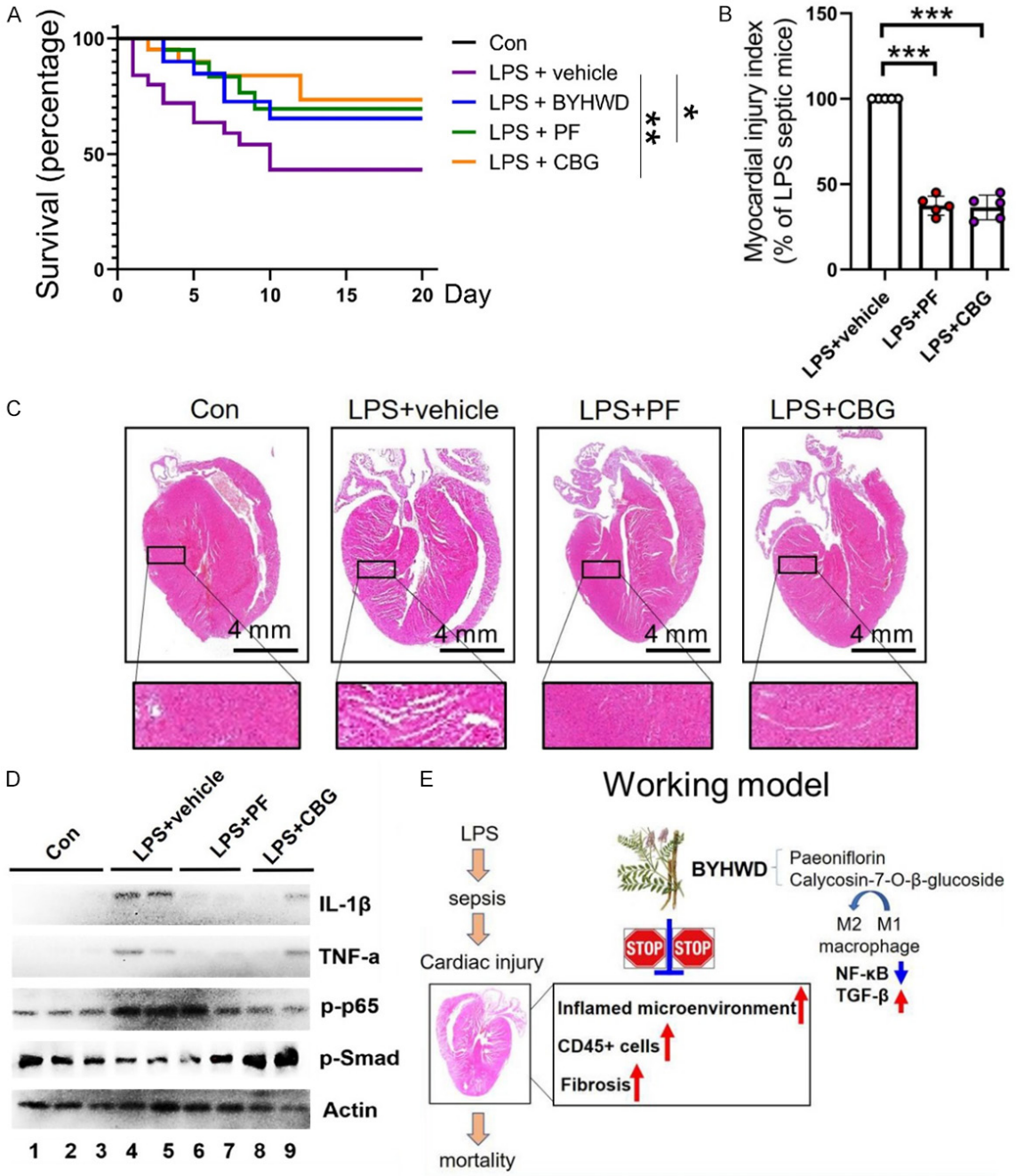

Figure 10. PF and CBG attenuate myocardial injury and improve survival of septic mice. A. The survival curves of normal (Con), vehicle, BYHWD (20 mg/Kg), PF (1.5 mg/Kg), and CGB (1 mg/Kg) treated LPS-induced septic mice (n

= 10 for each group). Log rank test. $^{*}P < 0.05$; $^{***}P < 0.001$. B. The myocardial injury index was quantified based on the crack number presented in myocardial tissues of vehicle, PF, and CBG treated septic mice (n = 5). C. H&E staining showing the myocardial histology of normal (Con) mice, and vehicle, BYHWD (20 mg/Kg), PF (1.5 mg/Kg), and CGB (1 mg/Kg) treated septic mice. Scale bar = 4 mm. D. Immunoblotting results showing the protein level of IL-1β, TNF-α, p-p65, p-Smad, and actin in the myocardial tissues of normal (Con) mice, vehicle, PF (1.5 mg/Kg), and CBG (1 mg/Kg)-treated septic mice. E. A schematic working model of the present study. BYHWD, with two key chemical components paeoniflorin (PF) and calycosin-7-O-β-glucoside (CBG), can mitigate SIMI by suppressing immune cell infiltration and promoting macrophage to acquire an M2-phenotype. Mechanistically, PF and CGB facilitate M2-macrophage phenotypic switch by coordinating NF-κB and TGF-β signaling pathways.

sis. This study has largely expanded the therapeutic repertoire of BYHWD particularly in SIMI, highlighting versatile roles of BYHWD as an old player on a new playground. We focus on the inflamed cardiac microenvironment in septic mice, providing promising translational values of BYHWD from bench to bedside.

Acknowledgements

This study was supported by Medical and health project (No. PKJ2021-Y02) of the special fund forlivelihood scientific research of Pudong New Area Scince and Technology Development Fund, Emergency Department of Integrated Traditional Chinese and Western Medicine, a key specialty inPudong New Area (No. PWZzk2022-15), and The BigDipper talent Training Program of Shanghai Seventh People's Hospital (No. BDX2021-03). These fundings were funded to Dr. Zhenyu Xu. This study was also funded by Talents Training Program of Shanghai Seventh People's Hospital, Shanghai University of Traditional Chinese Medicine (New Star, Grant No. 2019-18), the virus infection clinical research program (2023XG015), and the Science Development Program of Shanghai University of Traditional Chinese Medicine to Dr. Lingling Xiao. We thank Dr. Zhengshang Ruan at Xinhua hospital, school of medicine, Shanghai Jiao Tong University, for his constructive suggestions during the finalization of this manuscript.

Disclosure of conflict of interest

None.

Address correspondence to: Drs. Lingling Xiao, Lifen Zhang and Zhenyu Xu, Department of Emergency Medicine, Emergency Intensive Care Unit, Shanghai Seventh People's Hospital, The Seventh People's Hospital Affiliated to Shanghai University of Traditional Chinese Medicine, 358 Datong Road, Pudong, Shanghai 200137, China. Tel: +86-13167025769; Fax: +86-51322100; E-mail: xiaoling3625@163.com (LLX); zhlfq1005@sina.com (LFZ); zy20220222@sina.com (ZYX); Dr. Kai Zhang, State Key Laboratory of Oncogenes and Related Genes, Renji-Med-X Stem Cell Research Center, Ren Ji Hospital, Shanghai Cancer Institute, Shanghai Jiao Tong University School of Medicine, 160 Pujian Road, Pudong, Shanghai 200127, China. E-mail: zhangkai@alumni.sjtu.edu.cn

References

[1] Rumery K, Yunus F and Frishman WH. Myocardial depression in sepsis: beneficial adaptation or sequelae that requires treatment? Cardiol Rev 2020; 28: 256-261.

[2] Nedeva C. Inflammation and cell death of the innate and adaptive immune system during sepsis. Biomolecules 2021; 11: 1011.

[3] Frencken JF, Donker DW, Spitoni C, Koster-Brouwer ME, Soliman IW, Ong DSY, Horn J, van der Poll T, van Klei WA, Bonten MJM and Cremer OL. Myocardial injury in patients with sepsis and its association with long-term outcome. Circ Cardiovasc Qual Outcomes 2018; 11: e004040.

[4] Guo Y, Wu B, Chen Q and Min S. Parecoxib ameliorates renal toxicity and injury in sepsis-induced mouse model and LPS-induced HK-2 cells. Drug Dev Res 2022; 83: 659-668.

[5] Wang P, Feng Z, Sang X, Chen W, Zhang X, Xiao J, Chen Y, Chen Q, Yang M and Su J. Kombucha ameliorates LPS-induced sepsis in a mouse model. Food Funct 2021; 12: 10263-10280.

[6] Tanaka KA, Kurihara S, Shibakusa T, Chiba Y and Mikami T. Cystine improves survival rates in a LPS-induced sepsis mouse model. Clin Nutr 2015; 34: 1159-1165.

[7] Lin H, Wang W, Lee M, Meng Q and Ren H. Current status of septic cardiomyopathy: basic science and clinical progress. Front Pharmacol 2020; 11: 210.

[8] Krishnan K, Wassermann TB, Tednes P, Bonderski V and Rech MA. Beyond the bundle: clinical controversies in the management of sepsis in emergency medicine patients. Am J Emerg Med 2022; 51: 296-303.

[9] Lam SM, Lau AC, Lam RP and Yan WW. Clinical management of sepsis. Hong Kong Med J 2017; 23: 296-305.
[10] Gotts JE and Matthay MA. Sepsis: pathophysiology and clinical management. BMJ 2016; 353: i1585.
[11] McDonough KH and Virag JI. Sepsis-induced myocardial dysfunction and myocardial protection from ischemia/reperfusion injury. Front Biosci 2006; 11: 23-32.
[12] Angurana SK, Bansal A, Muralidharan J, Aggarwal R and Singhi S. Cytokine levels in critically ill children with severe sepsis and their relation with the severity of illness and mortality. J Intensive Care Med 2021; 36: 576-583.
[13] Wang L, Zhao H and Wang D. Inflammatory cytokine expression in patients with sepsis at an intensive care unit. Exp Ther Med 2018; 16: 2126-2131.
[14] Chousterman BG, Swirski FK and Weber GF. Cytokine storm and sepsis disease pathogenesis. Semin Immunopathol 2017; 39: 517-528.
[15] Pecoraro M, Del Pizzo M, Marzocco S, Sorrentino R, Ciccarelli M, Iaccarino G, Pinto A and Popolo A. Inflammatory mediators in a short-time mouse model of doxorubicin-induced cardiotoxicity. Toxicol Appl Pharmacol 2016; 293: 44-52.
[16] Belperio J, Horwich T, Abraham WT, Fonarow GC, Gorcsan J 3rd, Bersohn MM, Singh JP, Sonel A, Lee LY, Halilovic J, Kadish A and Shalaby AA. Inflammatory mediators and clinical outcome in patients with advanced heart failure receiving cardiac resynchronization therapy. Am J Cardiol 2016; 117: 617-625.
[17] Afanasyeva M, Wang Y, Kaya Z, Park S, Zilliox MJ, Schofield BH, Hill SL and Rose NR. Experimental autoimmune myocarditis in A/J mice is an interleukin-4-dependent disease with a Th2 phenotype. Am J Pathol 2001; 159: 193-203.
[18] Lee YS, Woo SC, Kim SY and Park JY. Understanding the multi-herbal composition of Buyang Huanwu Decoction: a review for better clinical use. J Ethnopharmacol 2020; 255: 112765.
[19] Jiang C, Xu YC, Zhang W, Pan W and Chao X. Effects and safety of Buyang-Huanwu Decoction for the treatment of patients with acute ischemic stroke: a protocol of systematic review and meta-analysis. Medicine (Baltimore) 2020; 99: e20534.
[20] Chen A, Wang H, Zhang J, Wu X, Liao J, Li H, Cai W, Luo X and Ju G. BYHWD rescues axotomized neurons and promotes functional recovery after spinal cord injury in rats. J Ethnopharmacol 2008; 117: 451-456.
[21] Kim KJ and Namgung U. Facilitating effects of Buyang Huanwu decoction on axonal regeneration after peripheral nerve transection. J Ethnopharmacol 2018; 213: 56-64.
[22] Chen S, Wang Y, Liang C, Li J, Li Y, Wu Q, Liu Z, Pang X and Chang YX. Buyang Huanwu Decoction ameliorates atherosclerosis by regulating TGF-beta/Smad2 pathway to promote the differentiation of regulatory T cells. J Ethnopharmacol 2021; 269: 113724.
[23] Yang DH, Ren XL, Xu F, Ma XQ, Liu GX, Li CH, Li C and Cai SQ. Absorptive constituents and their metabolites in drug-containing urine samples from Wuzhishan miniature pigs orally administered with Buyang Huanwu decoction. J Nat Med 2014; 68: 11-21.
[24] Yang J, Gao F, Zhang Y, Liu Y and Zhang D. Buyang Huanwu Decoction (BYHWD) enhances angiogenic effect of mesenchymal stem cell by upregulating VEGF expression after focal cerebral ischemia. J Mol Neurosci 2015; 56: 898-906.
[25] Yu P, Guan L, Zhou L, Guo J, Guo R, Lin R, Ding W, Li X and Liu W. Upregulation of glutamate metabolism by BYHWD in cultured astrocytes following oxygen-glucose deprivation/reoxygenation in part depends on the activation of p38 MAPK. Exp Ther Med 2017; 13: 3089-3096.
[26] Liu Y, Lin R, Shi X, Fang Z, Wang W, Lin Q, Zhang J, Zhang H and Ji Q. The roles of Buyang Huanwu Decoction in anti-inflammation, antioxidation and regulation of lipid metabolism in rats with myocardial ischemia. Evid Based Complement Alternat Med 2011; 2011: 561396.
[27] Xiao W, He Z, Luo W, Feng D, Wang Y, Tang T, Yang A and Luo J. BYHWD alleviates inflammatory response by NIK-mediated repression of the noncanonical NF-kappaB pathway during ICH recovery. Front Pharmacol 2021; 12: 632407.
[28] Cho DH, Ko SM, Son JW, Park EJ and Cha YS. Myocardial injury and fibrosis from acute carbon monoxide poisoning: a prospective observational study. JACC Cardiovasc Imaging 2021; 14: 1758-1770.
[29] Dartiguelongue JB. Systemic inflammation and sepsis. Part I: storm formation. Arch Argent Pediatr 2020; 118: e527-e535.
[30] Peng D, Fu M, Wang M, Wei Y and Wei X. Targeting TGF-beta signal transduction for fibrosis and cancer therapy. Mol Cancer 2022; 21: 104.
[31] Liamina SV, Vedenikin TIu, Borodovitsyna OA, Kruglov SV and Malyshev I. M1 and M2 macrophage phenotypes functional activity as essential components in innate immune response assessment. Ross Fiziol Zh Im I M Sechenova 2012; 98: 1030-1035.

[32] Yunna C, Mengru H, Lei W and Weidong C. Macrophage M1/M2 polarization. Eur J Pharmacol 2020; 877: 173090.
[33] Wen XD, Liu EH, Yang J, Li CY, Gao W, Qi LW, Wang CZ, Yuan CS and Li P. Identification of metabolites of Buyang Huanwu Decoction in rat urine using liquid chromatography-quadrupole time-of-flight mass spectrometry. J Pharm Biomed Anal 2012; 67-68: 114-122.
[34] Liu EH, Qi LW, Peng YB, Cheng XL, Wu Q, Li P and Li CY. Rapid separation and identification of 54 major constituents in Buyang Huanwu Decoction by ultra-fast HPLC system coupled with DAD-TOF/MS. Biomed Chromatogr 2009; 23: 828-842.
[35] Wang PC, Wang SX, Yan XL, He YY, Wang MC, Zheng HZ, Shi XG, Tan YH and Wang LS. Combination of paeoniflorin and calycosin-7-glucoside alleviates ischaemic stroke injury via the PI3K/AKT signalling pathway. Pharm Biol 2022; 60: 1469-1477.
[36] Han X, Zhang G, Chen G, Wu Y, Xu T, Xu H, Liu B and Zhou Y. Buyang Huanwu Decoction promotes angiogenesis in myocardial infarction through suppression of PTEN and activation of the PI3K/Akt signalling pathway. J Ethnopharmacol 2022; 287: 114929.
[37] Zhu JZ, Bao XY, Zheng Q, Tong Q, Zhu PC, Zhuang Z and Wang Y. Buyang Huanwu Decoction exerts cardioprotective effects through targeting angiogenesis via Caveolin-1/VEGF signaling pathway in mice with acute myocardial infarction. Oxid Med Cell Longev 2019; 2019: 4275984.
[38] Zhou YC, Liu B, Li YJ, Jing LL, Wen G, Tang J, Xu X, Lv ZP and Sun XG. Effects of Buyang Huanwu Decoction on ventricular remodeling and differential protein profile in a rat model of myocardial infarction. Evid Based Complement Alternat Med 2012; 2012: 385247.

Supplementary Table 1. Antibodies used in this study

Antibodies	Lot No.	Vendor
Col1a1	72026	Cell signaling technology
αSMA	Ab7817	Abcam
Cleaved caspase 3	9664	Cell signaling technology
γH2AX	Ab81299	Abcam
CD45	Ab10558	Abcam
IL1β	12242	Cell signaling technology
TNFα	A0277	Abclonal
p-Stat3	9145	Cell signaling technology
p-p65	3033	Cell signaling technology
p-Smad	13820	Cell signaling technology
p-p38	4571	Cell signaling technology
Actin	AC026	Cell signaling technology
Arg1	93688	Cell signaling technology
iNOS	13120	Cell signaling technology
CD45.2-PE	12-0451-82	invitrogen
CD11b-FITC	11-0112-41	invitrogen
F4/80-PerCP-Cy5.5	45-4801-82	invitrogen

Supplementary Table 2. Primer sequences for qPCR (5'-3')

Cd86	Forward: TCAATGGGACTGCATATCTGCC
	Reverse: GCCAAAATACTACCAGCTCACT
Actin	Forward: GGCTGTATTCCCCTCCATCG
	Reverse: CCAGTTGGTAACAATGCCATGT
H2Aa	Forward: GACCACGTAGGCACCTATGG
	Reverse: CTACAGCTATGTTTTGCAGTCCA
Tnf	Forward: CAGGCGGTGCCTATGTCTC
	Reverse: CGATCACCCCGAAGTTCAGTAG
Nos2	Forward: GTTCTCAGCCCAACAATACAAGA
	Reverse: GTGGACGGGTCGATGTCAC
Mcr1/Cd206	Forward: CAGAGCGATTACCTACCCAGC
	Reverse: ATTGGGGTTTACCGTGCTCAC
Cd163	Forward: GGTGGACACAGAATGGTTCTTC
	Reverse: CCAGGAGCGTTAGTGACAGC
Cd68	Forward: TGTCTGATCTTGCTAGGACCG
	Reverse: GAGAGTAACGGCCTTTTTGTGA
Arg1	Forward: CTCCAAGCCAAAGTCCTTAGAG
	Reverse: GGAGCTGTCATTAGGGACATCA

Supplementary Table 3. The botanical components of BYHWD

Chinese name	English name	Latin name	Family	Part used	Dry weight (g)
Huangqi	Astragali Radix	*Astragalus membranaceus (Fisch.) Bge. var. mongholicus* (Bge.) Hsiao or *Astragalus membranaceus* (Fisch.) Bge	Leguminosae	root	120
Chishao	Paeoniae Radix Rubra	*Paeonia lactiflora* PalL or *Paeonia veitchii* Lynch	Ranunculaceae	root	6
Danggui	Angelicae Sinensis Radix	*Angelica sinensis* (Oliv.) Diels.	Umbelliferae	Rhizome	4
Chuanxiong	Chuanxiong Rhizoma	*Ligusticum chuanxiong* Hort	Umbelliferae	root	5
Honghua	Carthami Flos	*Carthamus tinctorius* L.	Feverfew	flower	3
Taoren	Persicae Semen	*Prunus persica* (L) Batsch or *Prunus davidiana* (Carr.) Franch.	Rosaceae	seed	3
Dilong	Pheretima	*Pheretima aspergillum* (E. Perrier) or *heretima vulgaris* Chen or *Heretima guillelmi* (Michaelsen) or *heretima pectinifera* Mkhaeken	Megascolecidae	Whole body	3